Journal of Engineering Physics and Thermophysics, Vol. 82, No. 6, 2009

BURNING OF HYDROGENOUS MIXTURES IN THE MODEL OF AN INTERNAL-COMBUSTION-ENGINE CHAMBER

M. S. Assad, V. V. Leshchevich, V. N. Mironov, O. G. Penyazkov, K. L. Sevruk, and A. V. Skilond'

UDC 536.46:621.4

The integral characteristics of burning of stoichiometric and lean hydrogenous mixtures in a cylindrical chamber at initial pressures of 0.024 to 1 MPa have been investigated. The propagation of the flame has been visualized and the distributions of its velocity and the running parameters of burning have been obtained. It has been shown that in synthesis-gas-based mixtures, the flame front has a "cellular structure;" its characteristic dimension grows with propagation of the flame. A method for determining the shape factor, which makes it possible to explain certain experimental regularities of burning, has been proposed. The results of the work can be used in selecting the parameters of mixtures and combustion chambers of heat engines operating on modified fuels.

Keywords: *hydrogen, synthesis gas, internal-combustion engine, stoichiometric coefficient, flame structure, normal burning velocity.*

Introduction. The attractiveness of utilization of hydrogen in internal-combustion engines (ICEs) is determined by its environmental purity, the unlimited raw-material reserves, and good motor properties [1]. However, despite the indicated advantages, the use of pure hydrogen as an alternative fuel is limited at present [2].

As applied to car engines, the basic problems of utilization of hydrogen are associated with the overall dimensions, weight, complexity, and cost of systems of its storage on board the vehicle. To improve certain ICE indices (to increase the efficiency and to diminish harmful discharge) it is currently more acceptable to utilize hydrogen in small amounts in combination with other fuels. Therefore, the use of hydrogen as an addition to hydrocarbon fuels is the focus of many investigations [3–5]. Owing to the wide concentration limits of ignition and to the high rate of diffusion and velocity of propagation of the flame (an order of magnitude higher than those of most hydrocarbons), the introduction of hydrogen into the fuel can ensure qualitative power control, good mixture formation, approximation of the actual engine cycle to a theoretical one, and intensification and stability of the process of combustion of lean hydrocarbon-air mixtures [5–7].

However, the utilization of hydrogen in mobile facilities even as an addition to the basic fuel is limited by its high explosion and fire hazard and by the absence of a developed infrastructure (system for transportation, storage, and refueling of vehicles). Therefore, there can be another variant of realization of the advantages of hydrogen in which it is produced from a hydrocarbon fuel (gasoline, natural gas, liquefied gases, methanol, etc.) directly on board the vehicle, which eliminates the necessity of storing it. Production of synthesis gas (mixture of CO and H_2) directly from hydrocarbons is the most promising in this respect, since in this case the fuel is the same for the ICE and the synthesis-gas generator.

Experiments on utilization of new, including hydrogen-containing (hydrogenous), fuels are carried out on running engines as a rule; the basic recorded parameters are their power, fuel consumption, and content of harmful substances in exhaust gases. To more efficiently utilize hydrogen one must study its influence on the process directly in the combustion chamber. The reason is that the use of hydrogen as the basic or constituent part of fuel produces changes in the working process that are caused by the decrease in the fuel-combustion time. The high velocity of propagation of the flame is a factor aiding in increasing the efficiency of the working process (engine efficiency) but bringing about very high rates of rise in the pressure in the engine's cylinder, which is undesirable, since it is mainly responsible for the rigid operation of the engine. The rate of rise in the pressure is determined by the composition of

A. V. Luikov Heat and Mass Transfer Institute, National Academy of Sciences of Belarus, 15 P. Brovka Str., Minsk, 220072, Belarus. Translated from Inzhenerno-Fizicheskii Zhurnal, Vol. 82, No. 6, pp. 1031–1045, November–December, 2009. Original article submitted March 20, 2009.

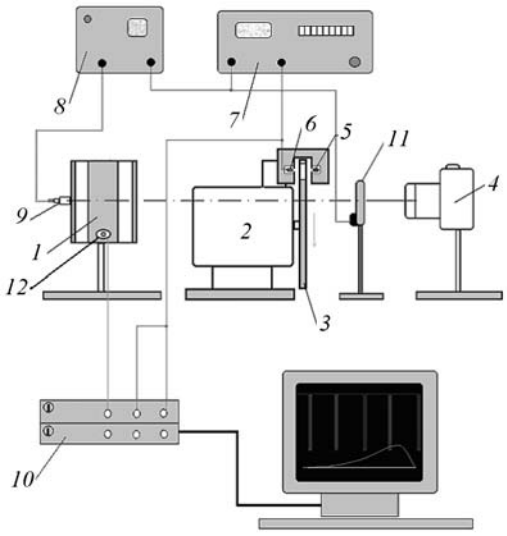

Fig. 1. Diagram of the experimental setup (version of central ignition): 1) combustion chamber; 2) electric motor; 3) disk with one or four slits; 4) digital photocamera; 5) light-emitting diode (LED); 7) delay former; 8) ignition-pulse former; 9) initiator (plug); 10) digital oscilloscope; 11) electromechanical shutter; 12) pressure transducer.

the fuel and by the velocity of propagation of the flame (burning velocity) u and the area of its surface S. The burning velocity can be controlled by changing the composition of the fuel and its excess coefficient (stoichiometric coefficient) and the initial pressure of the mixture P_0, whereas the size of the flame surface can be controlled by the geometric shape of the combustion chamber and the location of the ignition initiator. All the above determined the objectives of this investigation. In the work, we study the burning of stoichiometric and lean mixtures with addition of hydrogen to the basic fuel (propane) and those based on hydrocarbon-conversion products (synthesis gas). Not only is the initial pressure of the mixtures varied but the site of their ignition is varied as well.

Experimental Setup. A diagram of the setup is presented in Fig. 1. Investigations were carried out in a model combustion chamber made of St45 steel with an inside diameter of 80 and a height of 32 mm; one end of the chamber was manufactured from quartz glass. The chamber's outside diameter was 144 mm. The mixture was ignited using a spark plug installed in the cylindrical wall (lateral ignition L) or at the center of the end wall (central ignition C). A PCB Piezotronics sensor, model 133A22, arranged in the chamber's cylindrical wall was used to record changes in pressure in the process of burning. In the experiments, we determined, in particular, two indices: the maximum pressure P_{max} developed in the chamber in the process of burning and the burning time of the mixture t_b (from the instant of ignition to attaining the pressure P_{max}) which are, in essence, the characteristics of the ICE operating cycle.

Burning in the chamber was visualized by the high-speed-photography method. The positions of the flame front were recorded from the instant of opening of the electromechanical shutter of a Canon EOS 300D digital camera through narrow slits of a disk rotating with a prescribed velocity (Fig. 1).

The delay between the instant of ignition of the mixture and the beginning of photorecording was set using a GZI-6 delayed-pulse oscillator and an I1-8 time-shift source, which were triggered on arrival of an electric pulse from the control light-emitting diode (LED). The control pulse was also used for synchronization of the triggering of a digital oscilloscope, which recorded signals from the detecting photodiode and the pressure transducer. The number of recorded positions of the flame front was determined by the time of opening of the electromechanical shutter, the number of slits on the disk, and its rotational velocity. The procedure of calculation of the running values of the flame-front velocity (burning velocity) in the chamber has been presented in [8].

Composition of the Investigated Mixtures. We used propane as the model hydrocarbon fuel. Stoichiometric and lean propane-air mixtures and mixtures of propane with air (containing 2 or 4 vol. % of hydrogen) which modeled the composition of the fuel on addition of hydrogen into the ICE air path were studied. Furthermore, we investigated, as the fuel, a mixture produced in the reaction of incomplete oxidation of propane (synthesis gas):

TABLE 1. Investigated Stoichiometric and Lean Fuel Mixtures

Fuel mixture	Initial fuel	Fuel-excess coefficient	Chemical composition	Mole content of hydrogen, %	Initial pressure, MPa
1	Propane	1.0	$C_3H_8 + 5O_2 + 18.81N_2$	–	0.1–1.0
1a	Propane	0.8	$0.8C_3H_8 + 5O_2 + 18.81N_2$	–	0.06–0.8
2	Propane, hydrogen	1.0	$C_3H_8 + 0.51H_2 + 5.26O_2 + 19.76N_2$	1.9	0.03–1.0
2a	Propane, hydrogen	0.8 for propane	$0.8C_3H_8 + 0.51H_2 + 5.26O_2 + 19.76N_2$	1.9	0.04–1.0
3	Propane, hydrogen	1.0	$C_3H_8 + 1.1H_2 + 5.54O_2 + 20.85N_2$	3.9	0.024–0.9
3a	Propane, hydrogen	0.8 for propane	$0.8C_3H_8 + 1.1H_2 + 5.54O_2 + 20.85N_2$	3.9	0.03–0.9
4	Propane-conversion products	1.0	$CO + 1.33H_2 + 1.17O_2 + 6.27N_2$	13.6	0.1–1.0
4a	Propane-conversion products	0.8 for conversion products	$0.8(CO + 1.33H_2 + 1.88\ N_2) + 1.17O_2 + 4.39N_2$	11.9	0.024–1.0

$$C_3H_8 + 1.5O_2 + 5.64N_2 \rightarrow 3CO + 4H_2 + 5.64N_2 . \quad (1)$$

The compositions of the fuel mixtures used in the experiments and the studied ranges of initial pressures are given in Table 1. The initial temperature of the mixtures was 290–300 K.

Integral Characteristics of Burning. The dependences of pressure in burning of the investigated mixtures and data on the maximum pressures in the chamber in their combustion have been given in [8, 9]. It has been noted that in stoichiometric burning, the maximum pressures in the mixtures with small additions of hydrogen (mixtures 2 and 3) slightly (to 2%) exceed the pressures in combustion of the model (propane-air) mixture 1, whereas in burning of synthesis-gas-based mixtures (mixture 4), P_{max} values are 13–15% lower than those for the model mixture because of the smaller available volume heat of combustion and the considerable amount of ballast nitrogen left in the mixture after the reaction of incomplete oxidation.

Another trend is observed in burning of lean fuel-air mixtures. The maximum pressure in the chamber in burning of synthesis gas is 3.5–10% (depending on P_0) higher than that in combustion of propane but lower than in hydrogen-enriched mixtures (2a and 3a). The reason for such behavior will be discussed below in analyzing experiments on burning vitalization.

Figure 2 gives the burning times of the investigated stoichiometric and lean mixtures as functions of the initial pressure in lateral ignition. The results are grouped into series with different sizes of the interelectrode gap of the plug. As the mixture's initial pressure increases, the optimum gap ensuring a more stable ignition of the mixtures diminishes. The higher the pressure, the more difficult the breakdown of the interelectrode gap; the lower the pressure, the larger the mixture's volume that must be heated to initiate burning [10]. In the investigated interval of initial pressures P_0 of 0.02 to 1.0 MPa, we carried out the experiments for a plug gap of 2.8 to 0.4 mm respectively. The experimental results for the interelectrode gaps that are optimum for each mixture and initial pressure can be satisfactorily approximated, as a rule, by the curves general for this mixture.

As could be expected, among the stoichiometric mixtures, the burning times of propane are the longest; the combustion time of the propane-air mixture grows almost linearly with initial pressure from 39 msec at P_0 = 0.11 MPa to 55 msec at P_0 = 0.96 MPa (Fig. 2a). Small additions of hydrogen exert a fairly strong influence on the burning time (Fig. 2b and c). Thus, on addition of 4% hydrogen to air (mixture 3), the burning time diminishes by 20–23% compared to the case of the burning of the model mixture. Qualitatively the form of the dependence on the initial pressure of the mixture remains the same. The synthesis-gas-based mixture burns up much faster than the model mixture under equivalent conditions (Fig. 2d); its burning time is 2.2–2.8 times shorter than that of the propane-air mixture. Furthermore, it is almost independent of the initial pressure in the combustion chamber.

Changeover from stoichiometric mixtures to lean ones has the most substantial effect on the burning of propane. Let us dwell, e.g., on the burning time as a function of the initial pressure of the mixture. If the decrease in the mixture's stoichiometric coefficient φ to 0.8 produces a 47% increase in the burning time at P_0 = 0.108 MPa, at 0.78 MPa, the increase is 90% now. Addition of hydrogen leads to a weakening of this dependence, with it being more substantial at elevated pressures. Thus, whereas at 0.108 MPa, the decrease in φ to 0.8 produces an increase of 35%

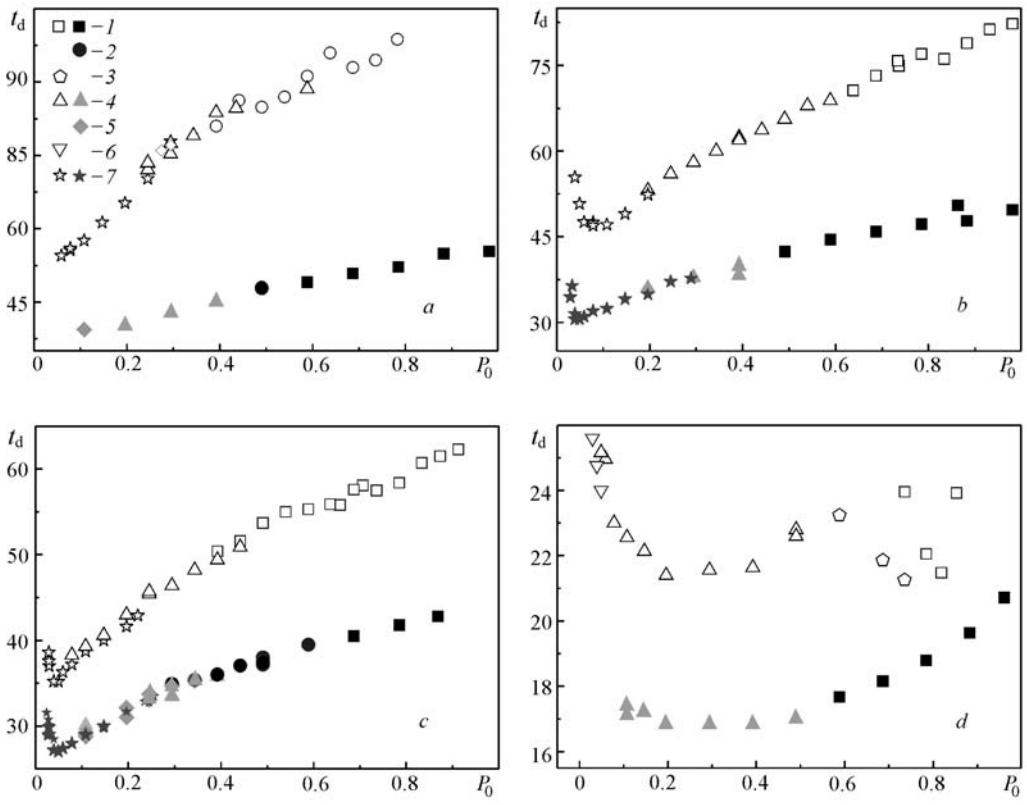

Fig. 2. Burning times of mixtures in lateral ignition vs. initial pressure in the chamber: a) mixtures 1 and 1a; b) 2 and 2a; c) 3 and 3a, and d) 4 and 4a (dark symbols, φ = 1, contour symbols, 0.8; 1) the spark-plug gap is 0.4, 2) 0.55, 3) 0.8, 4) 1.0, 5) 1.5, 6) 2.0, and 7) 2.8 mm). P_0, MPa; t_b, msec.

in the burning time of mixture 3a compared to the stoichiometric mixture, at 0.78 MPa, the increase is 38%, i.e., with a content of about 4% hydrogen in the mixture, the growth in the burning time is nearly independent of the initial pressure.

Thus, in the range of the investigated pressures, the presence of molecular hydrogen ensures a more substantial action on the burning velocity of propane-air mixtures in the case of lean mixtures than in the case of stoichiometric mixtures. Thus, at an initial pressure of 0.8 MPa, addition of 4% hydrogen produces a decrease of 1.25 times in the burning time of the mixture of propane with air in the case of the stoichiometric composition and of 1.7 times now for φ = 0.8. This suggests the possibility of increasing the indicator (inside the cylinder) efficiency due to additions of hydrogen for the regimes of ICE operation on lean mixtures. Therefore, when a propane-butane- or gasoline-fueled engine is modernized, it is most expedient to increase the burning velocity (by watering down the air entering the engine) precisely in the regimes of operation on lean mixtures, in particular, under municipal-operation conditions.

With allowance for the marked influence of even small additions of hydrogen on the process of burning of propane, it is clear that the behavior of synthesis-gas-based mixtures (where the fraction of H_2 is a third larger than the CO fraction and amounts to nearly 14% in stoichiometry) must differ from the behavior of the model mixture even more significantly. In the range of initial pressures to 0.4 MPa, the burning times of these mixtures diminish as P_0 grows. The relative decrease in the burning time is virtually independent (in the investigated limits) of the stoichiometric coefficient φ and amounts to about 5% with variation in the pressure from 0.108 to 0.39 MPa. Interestingly, in the above range, the increase in the burning time with changeover to a lean mixture is P_0-independent and amounts to 28% with variation in φ from 1 to 0.8. These data correlate well with the results obtained for hydrogen-enriched mixtures. As has been noted, for a hydrogen fraction of about 4% in the mixture, the growth in the burning time is virtually independent of the initial pressure in the range 0.108–0.78 MPa and amounts to 35–38% with variation in φ from 1 to 0.8.

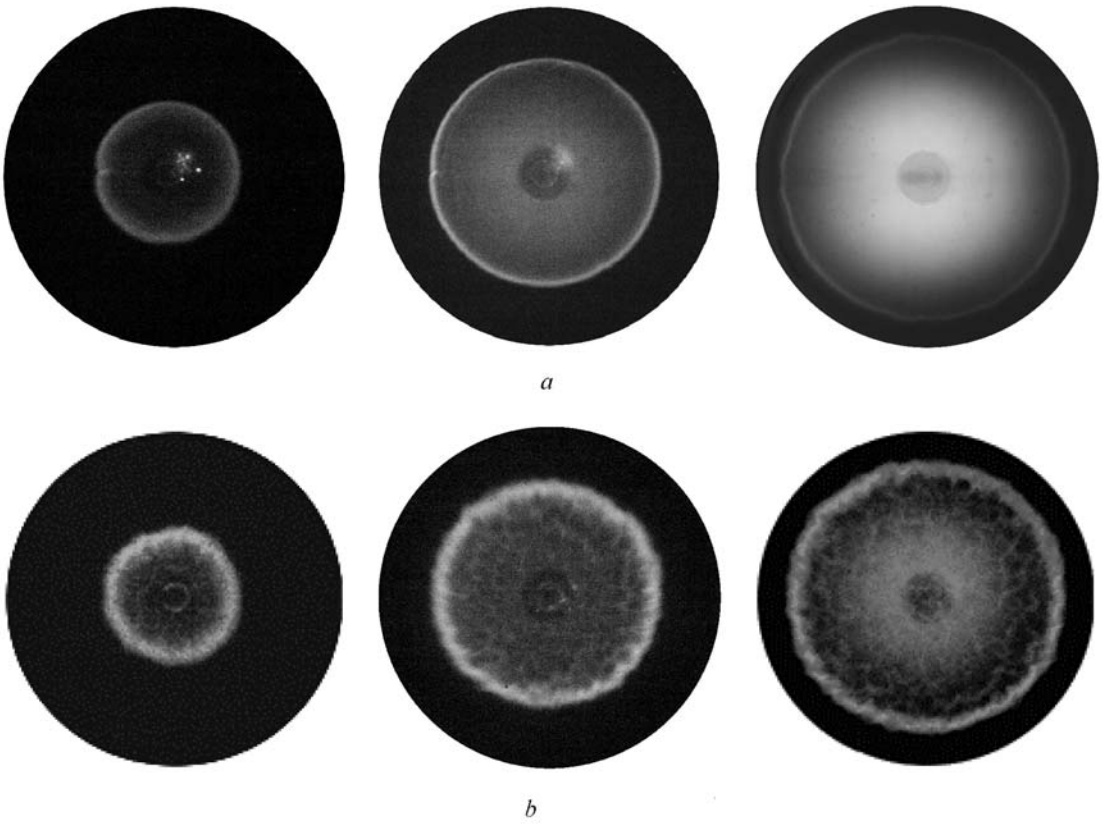

Fig. 3. Photographs of the positions of the flame front in lean mixtures in central ignition and at an initial pressure of 0.491 MPa: a) mixture 2a within 10.1, 20.1, and 30 msec from the instant of initiation; b) mixture 4a within 4.7, 8.6, and 11 msec from the instant of initiation.

Burning-Visualization Results. Visualization of burning in different mixtures under different ignition conditions has made it possible to reveal the characteristic features of propagation of the flame front. The dynamics of burning processes for the cases of lateral and central ignition has been considered in [9]. In the present work, Fig. 3 compares the character of propagation of the flame for a 2% hydrogen-enriched propane-air mixture and a synthesis-gas-based mixture ($\varphi = 0.8$ in both cases). It is seen that whereas in mixture 2a, the burning is nearly laminar in character with a smooth flame front, in mixture 4a, we observe a cellular structure of the flame front, which is different from that observed in burning in soap bubbles at constant pressure [11]. The characteristic dimension of the cells grows with time nearly in proportion to the distance between the front and the point of initiation of burning. The presented photographs (Fig. 3b) demonstrate the front structure in central ignition of a lean synthesis-gas-based mixture. We note that the above structure was found earlier in burning of the corresponding stoichiometric mixture 4; also, it is pronounced in the case of lateral initiation.

Individual photographs of the process of burning are similar to those presented in [12] where the stability of a spherical flame front in rich ($\varphi = 1.25$) propane-air mixtures has been investigated; however, the dynamics of the process in a synthesis-gas-based mixture is closer to that presented in [13, 14] where the burning of a binary fuel ($H_2 + CO$) has been studied in a spherical bomb. Whereas in [12], disturbances on the flame surface develop, then break and form a fine cellular structure, in lean mixtures of a binary fuel ($CO/H_2 = 1$) and in mixtures 4 and 4a of this work, cells grow with time and attain, by the end of the process, a dimension just an order of magnitude smaller than the chamber diameter in our case.

During the processing of the photographs, we determined the distances traversed by the combustion front from the site of ignition and the velocities of propagation of the flame front u as functions of the time and along the diameter or on the radius of the combustion chamber. Part of the obtained results is presented in Figs. 4–6. Also, these

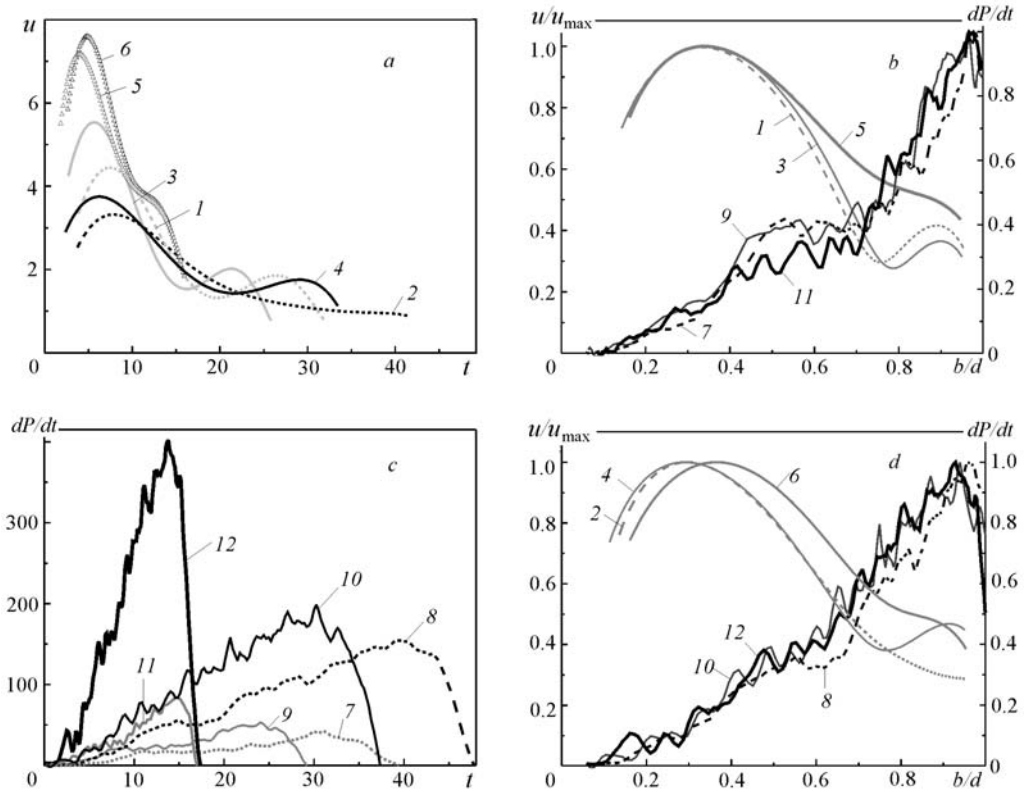

Fig. 4. Curves of the velocity of propagation of the flame u (1–6) and the rate of change in the pressure dP/dt (7–12) in burning of stoichiometric mixtures with time (a and c) and in the process of motion of the combustion front along the chamber diameter (b and d) and in the case of lateral ignition: 1, 2, 7, and 8) mixture 1; 3, 4, 9, and 10) mixture 3; 5, 6, 11, and 12) mixture 4; odd figures, at P_0 = 0.108 MPa, even figures, at 0.491 MPa. t, msec; u, m/sec; dP/dt, MPa/sec.

figures show the dynamics of variation in the pressure and the curves of the rate of rise in the pressure dP/dt in the combustion chamber, whose analysis is given below, just as an analysis of other local characteristics of burning of hydrogeneous mixtures.

For the sake of convenience, part of the results is presented in dimensionless form; the values of the functions are normalized to their maximum values, and those of the arguments are normalized to the dimensions of the combustion chamber (d = 80 mm and r_{ch} = 40 mm for the versions of lateral and central ignition respectively). The maxima of the functions (indices of burning of fuel mixtures) are presented in Table 2. In addition to the already indicated indices P_{max} and t_b, the table gives the maximum flame velocity u_{max}, the maximum rate of rise in the pressure $(dP/dt)_{max}$, and the time of reaching it from the instant of initiation $t_{(dP/dt)_{max}}$, the equilibrium pressure P_{eq}, and the ratio of the maximum pressure to the initial one P_{max}/P_0, of the equilibrium pressure to that initial P_{eq}/P_0, and of the maximum one to that equilibrium P_{max}/P_{eq}. Calculations of the equilibrium values of the pressure P_{eq} were carried out for the case of adiabatic burning of mixtures of a prescribed composition at constant volume with the Chemical Equilibrium (CE) program developed on the basis of a well-known program package [15] and using the thermodynamic data from [16]. In the calculations, we used the Chem05VERS.bin database including data on 127 components.

The chamber's space where the front velocities were determined did not include the region with a weak luminous emittance of the flame and the region of the final stage of burning (because of the difficulty of establishing the front shift between exposures). Owing to this, the measurement error for velocity was usually no higher than 7–12% (for different mixtures).

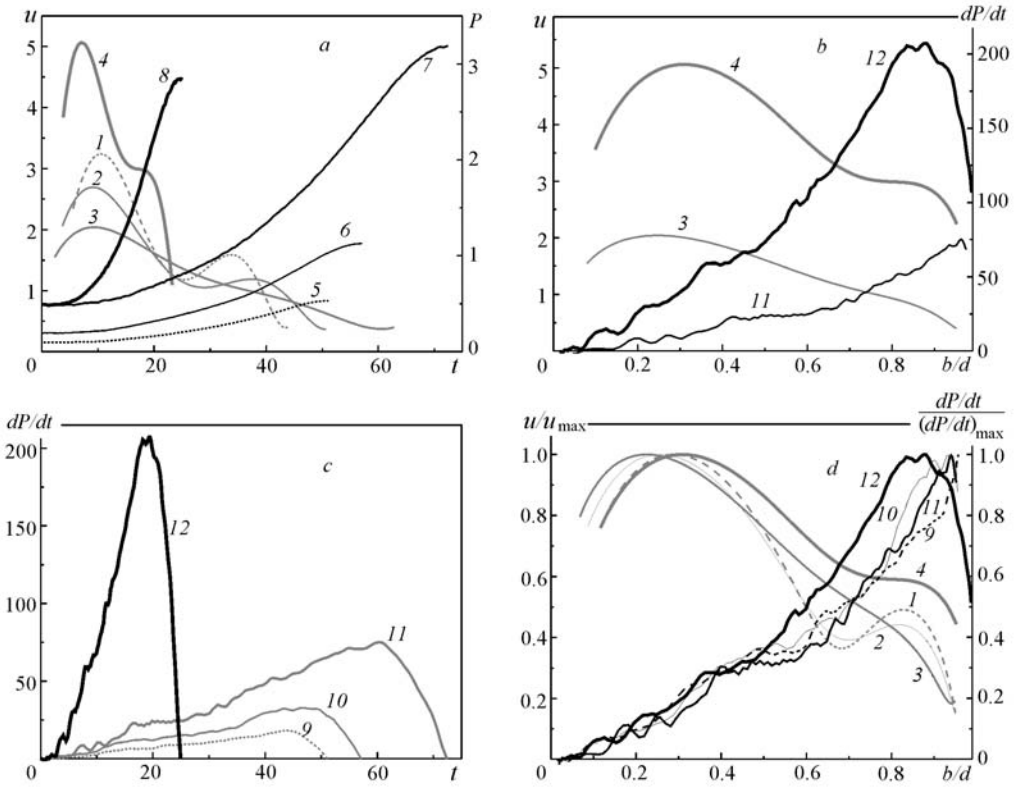

Fig. 5. Curves of the velocity of propagation of the flame u (1–4) and the pressure P (5–8) and the rate of change in the pressure dP/dt (9–12) in burning of lean mixtures with time (a and c) and along the chamber diameter (b and d) in the case of lateral ignition: 1, 5, and 9; 2, 6, and 10; 3, 7, and 11) mixture 2a at P_0 = 0.108, 0.196, and 0.491 MPa respectively; 4, 8, and 12) mixture 4a at P_0 = 0.491 MPa. t, msec; u, m/sec; P, MPa; dP/dt, MPa/sec.

Analysis of the Indices of Burning. An analysis of the results presented in Table 2 makes it possible to generalize, to the case of central ignition, the already discussed dependences of the integral characteristics of burning P_{max} and t_b on the initial pressure of mixtures, such as an increase in the maximum pressure in the chamber with P_0 and an increase in the burning time t_b in a model mixture and its hydrogen-enriched modifications at $P_0 \gtrsim 0.1$ MPa. The actual independence of the burning time from P_0 has also been confirmed for synthesis gas-based mixtures. The indicated regularities are true for both stoichiometric and lean mixtures given in Table 2.

It should be noted that for all of the presented mixtures and versions of ignition, the values of P_{max} grow faster than their initial pressures. Thus, in case of $\varphi = 1$, when P_0 grows 4.5 times, the maximum burning pressures increase more than 5 times; for lean mixtures, an increase of 5 times in the initial pressure results in P_{max} growing 5.7–6.0 times, with the last value being practically independent of the site of the initiation of burning. The values of $P_{max}(P_0)$ were averaged for each P_0 on the basis of more than ten experiments; therefore, the peculiarities in the behavior of the dependences $P_{max}(P_0)$ are determined rather accurately. It is seen that for all versions of the process, the values of P_{max}/P_0 increase as P_0 grows and approach the calculated values of P_{eq}/P_0.

The factor that determines the growth in the P_{max}/P_0 ratio with initial pressure, in our view, is the heat exchange between the chemically reacting mixture and the walls of the combustion chamber. The most probable cause of the pressures P_{max} in the chamber approaching P_{eq} is a decrease in the share of the moisture being condensed on contact with the walls as P_0 increases. The increase in energy release leads to deeper local heating of the surface layers of the chamber walls which, due to this, despite the incommensurable coefficients of heat transfer of the wall's metal and the combustion products, indeed cool down at a slower rate. This in turn prevents water condensation leading to a reduction in the partial pressure of the steam and the total pressure of the gas medium in the combustion chamber.

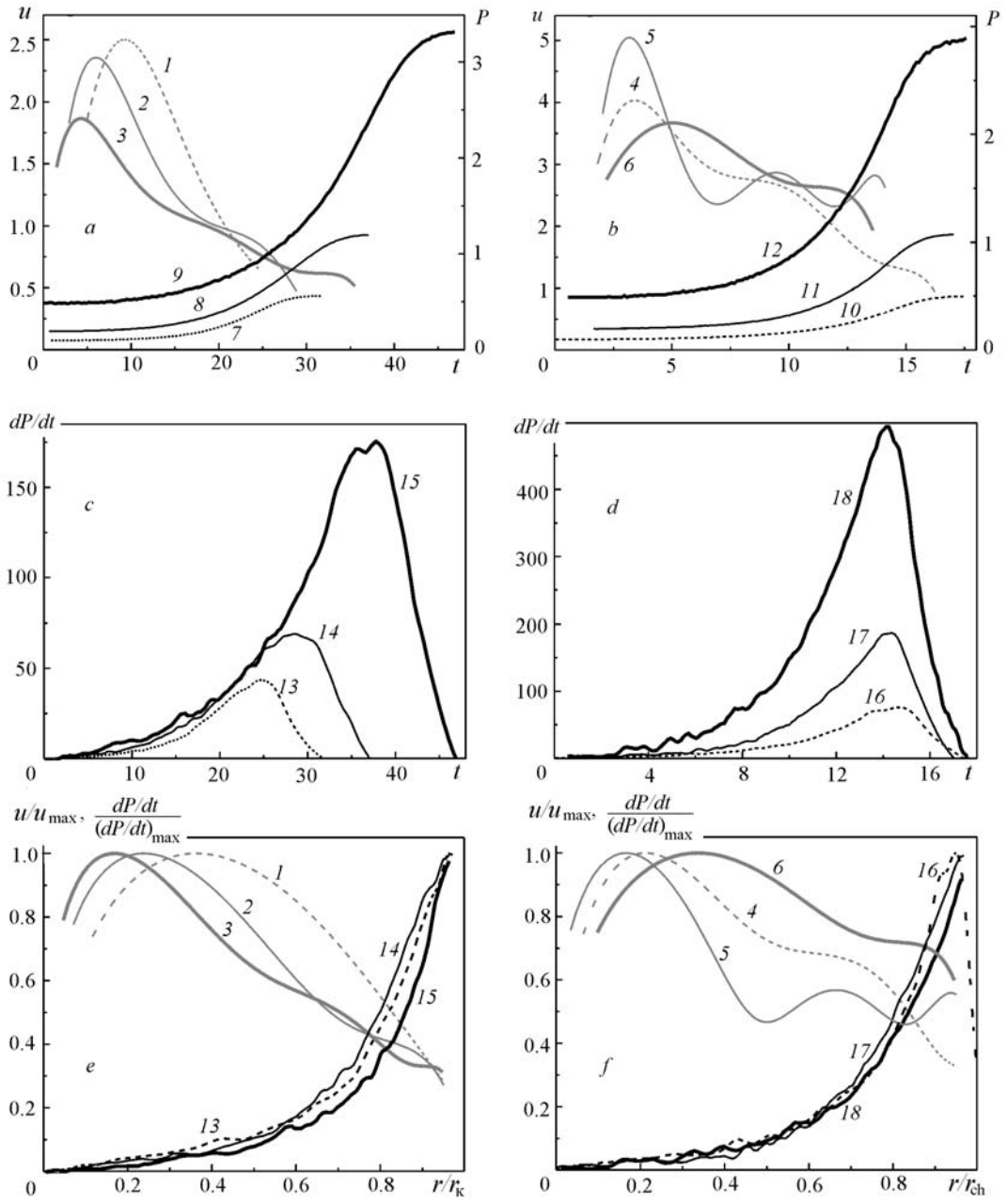

Fig. 6. Curves of the velocity of propagation of the flame u (1–6) and the pressure P (7–12) and of the rate of change in the pressure dP/dt (13–18) in burning of lean mixtures with time (a and b, c and d respectively), and the dimensionless dependences of the above velocity and rate on the dimensionless flame radius (e and f) in the case of central ignition in mixtures 2a (1–3, 7–9, and 13–15) and 4a (4–6, 10–12, and 16–18) at P_0 = 0.108, 0.196, and 0.491 MPa in order of increasing figures in the groups. t, msec; u, m/sec; P, MPa; dP/dt, MPa/sec.

The data in Table 2 confirm once again that an insignificant addition of hydrogen to the model mixture has practically no effect on the value of the ratio P_{max}/P_0, but leads to a noticeable reduction in the burning time (mixtures 1 and 3). The values of P_{max}/P_0 are also insignificantly affected by the site of ignition (although when initiated at the center, P_{max}/P_0 are always higher). Thus, when φ = 0.8 the values P_{max}/P_0 practically coincide in mixture 4a and differ by 5–6% in mixture 2a.

TABLE 2. Indices of Burning of Fuel Mixtures in Experiments with Visualization

Fuel ignition	Ignition	P_0, MPa	t_b, msec	u_{max}, m/sec	P_{max}, MPa	P_{eq}, MPa	P_{max}/P_0	P_{eq}/P_0	P_{max}/P_{eq}	$(dP/dt)_{max}$, MPa	$t_{(dP/dt)_{max}}$, msec
1	L	0.108	39.4	4.5	0.82	1.02	7.6	9.4	0.80	42	31
	L	0.491	47.8	3.3	4.17	4.75	8.5	9.7	0.88	155	39
3	L	0.108	29.2	5.5	0.84	1.01	7.8	9.4	0.83	53	24
	L	0.491	37.3	3.8	4.21	4.66	8.6	9.5	0.90	199	30
4	L	0.108	17.0	7.2	0.72	0.81	6.7	7.5	0.89	84	15
	L	0.491	17.4	7.6	3.63	3.72	7.4	7.6	0.98	404	14
2a	L	0.098	51.1	3.2	0.53	0.84	5.4	8.6	0.63	18	44
	L	0.196	57.1	2.7	1.13	1.69	5.8	8.6	0.67	33	47
	L	0.491	72.4	2.0	3.19	4.24	6.5	8.6	0.75	75	56
	C	0.098	31.8	2.5	0.56	0.84	5.7	8.6	0.67	44	25
	C	0.196	37.1	2.4	1.20	1.69	6.1	8.6	0.71	69	29
	C	0.491	46.9	1.9	3.31	4.24	6.7	8.6	0.78	176	38
4a	L	0.491	25.0	5.1	2.86	3.50	5.8	7.1	0.82	207	19
	C	0.098	17.4	4.0	0.50	0.70	5.1	7.1	0.71	76	15
	C	0.196	17.0	5.0	1.07	1.40	5.5	7.1	0.76	187	14
	C	0.491	17.6	3.7	2.89	3.50	5.9	7.1	0.83	493	14

Comparison of the values of maximum flame-propagation velocities given in Table 2 shows that in the same versions of ignition, high values of u_{max} correspond to shorter burning times t_b. However the obvious connection between these indices of burning is not always accompanied by quantitative agreement, especially for different mixtures. Thus, in case of lateral ignition and P_0 = 0.108 MPa when the ratio of the maximum velocities in mixtures 4 and 1 is 1.6, the burning time of a model mixture is 2.3 times longer than that of a synthesis-gas-based mixture. In the case of central ignition and P_0 = 0.491 MPa the ratio of the maximum velocities in mixtures 4a and 2a is 1.9, and their burning times differ 2.7 times. It is to explain these facts and to analyze the peculiarities in the burning of different mixtures that the following part of the work is devoted to.

Local Characteristics of Burning. *Stoichiometric Mixtures.* Figure 4 gives the time dependences of the flame velocity u, the rate of rise in the pressure dP/dt, and their change as the front moves along the diameter of the combustion chamber in mixtures 1, 3, and 4. It is significant that the velocity u is not stationary and markedly changes with time and along the chamber diameter. In mixtures 1 and 3, in addition to the principal velocity maximum falling on the initial stage of burning, we observe the second, weaker maximum as a rule. In mixture 3 containing about 4% hydrogen, the second maximum is pronounced at both initial pressures, whereas in the model mixture 1, the second velocity maximum is absent at a higher P_0.

The second maxima are absent from the fast burning synthesis-gas-based mixture 4, but the descending branches of the curves have characteristic portions where the reduction in the velocity slows down. It is seen that in this mixture, the flame velocities are nearly coincident along the length of the combustion chamber at initial pressures of 0.108 and 0.491 MPa. Thus, the dynamics of burning of mixture 4 is weakly dependent on pressure even in the details.

The family of u_j curves collected in Fig. 4a seems weakly correlated. However, if we represent the data in the form of dimensionless dependences $u_j/u_{j_{max}} = f(b/d)$ (where b is the distance diametrally traversed by the combustion front and d is the chamber diameter), the correlation of the obtained results is beyond question (Fig. 4b and d). At a lower initial pressure, the positions of the principal maxima of all curves are coincident. The positions of the second maxima are close, and the portion of reduction in the velocity in the synthesis-gas mixture 4 is close in location to the minima of the functions for the model and hydrogen-enriched mixtures 1 and 3. For both P_0 values, the veloc-

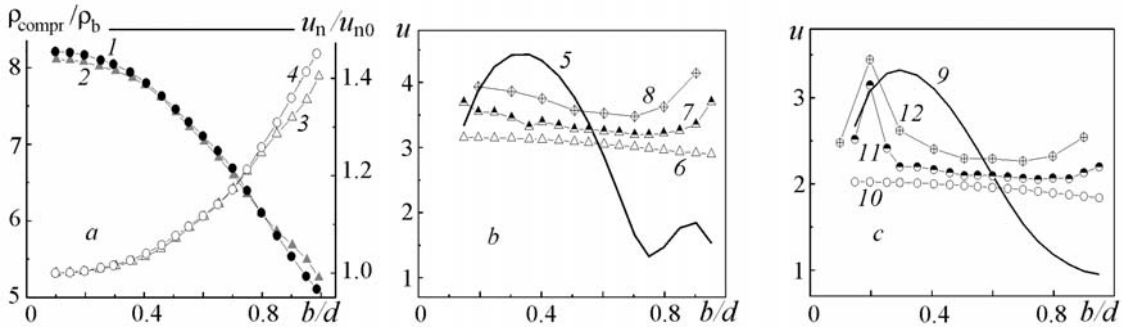

Fig. 7. Distribution of the burning parameters in the chamber in lateral ignition in the stoichiometric propane-air mixture at the initial pressure P_0 = 0.108 MPa (1, 3, and 5–8) and 0.491 (2, 4, and 9–12): 1 and 2) ρ_{compr}/ρ_b; 3 and 4) u_n/u_{n_0}; 5 and 9) data from Fig. 4; 6 and 10) calculation using the Chemical Equilibrium program; 7 and 11) the same, with allowance for F for subdivision into 20 regions; 8 and 12) the same, with allowance for F for subdivision into 10 regions. u, m/sec.

ity maxima in mixture 4 are broader than those in mixtures 1 and 3, i.e., higher flame velocities in mixture 4 are realized in a larger combustion-chamber space.

We consider qualitatively what causes the distribution of the reduced burning velocities, which is presented in Fig. 4b and d (at an initial pressure of 0.108 and 0.491 MPa respectively). Let us assume that the combustion front is spherical and, following [10], write a relationship between the velocity of propagation of the flame u and the normal burning velocity u_n in the following form:

$$u = \frac{\rho_{compr}}{\rho_b} u_n , \tag{2}$$

where ρ_{compr} and ρ_b are the density of the compressed fresh mixture and the combustion products respectively.

We evaluate how the factors of expression (2) change. The normal burning velocity is the physicochemical index of a fuel mixture and, e.g., for a stoichiometric mixture of propane with air under normal conditions, we have u_{n_0} = 0.4 m/sec [10]. The quantity u_n is dependent on the pressure and temperature of the fuel mixture; for hydrocarbons, these dependences have the following form [10]:

$$u_n \sim P^m , \tag{3}$$

$$u_n \sim T^{1.8} . \tag{4}$$

Here m is the empirical parameter related to the effective reaction order. For slowly burning mixtures (u_n < 0.4–0.5 m/sec), we have m < 1, i.e., growth in the pressure leads to a decrease in u_n; for fast-burning mixtures of hydrocarbons and CO with air, the quantity m is equal to –(0.25–0.30) [17]. For propane at φ = 1.04, we have m = –0.3 [10]. It is significant that within 373–723 K, the quantity m is weakly dependent on temperature [10], i.e., dependences (3) and (4) can be assumed to be uncorrelated. In this case, e.g., with isothermal increase in P_0 from 0.108 to 0.491 MPa, the normal velocity of burning of the model mixture 1 will diminish by 36%, whereas with isobaric increase in the fresh-mixture temperature from 293 to 441 K, it will grow 2.1 times. Therefore, in a nearly adiabatic compression of the fresh mixture in the chamber, the normal burning velocity will always grow.

If the combustion-chamber volume is subdivided into a number of regions whose boundaries will be the surfaces of the flame front and the chamber walls [18], the process of burning in each will be nearly isobaric. It is precisely for this reason that the quantity $(\rho_{compr_i}/\rho_{b_i}) \sim (T_{b_i}/T_{compr_i})$ can be approximately calculated in each region (e.g., using the CE program) for the case of burning at constant pressure. Calculations of the $(\rho_{compr_i}/\rho_{b_i}) = f(b/d)$

distribution in burning of the stoichiometric propane-air mixture are presented in Fig. 7a; the same figure gives the $(u_n/u_{n_0}) = g(b/d)$ distributions for the adiabatically compressed mixture with allowance for dependences (3) and (4). Figure 7b and c shows the burning-velocity distributions in the chamber at initial pressures of 0.108 and 0.491 MPa respectively. It is seen that the calculated distributions differ significantly from those obtained experimentally. Their difference is caused by the form of the u (u_n) dependence, which has been adopted according to (2); this dependence corresponds to the case of the propagation of burning with a spherical front from the origin of coordinates in an arbitrary solid angle Ω. With such geometry the combustion products are stationary. Then we obtain

$$dV(\Omega) + S(\Omega)\, dR\,, \tag{5}$$

where V is the volume of the combustion products, S is the burning surface (area), and R is the radius of the flame front.

In our case the flame-front surface is bounded by the regions of intersection of the space and the chamber walls (see [19]) and it is necessary to allow for the departure of the chamber shape from the case of burning in the region Ω = const. Let us introduce the discrete function $F_i(b_i/d)$, i.e., the shape factor, determining it as follows:

$$F_i = \frac{\Delta V_{\text{sph}i}\,(b_i/d)}{\Delta V_i\,(b_i/d)}\,, \tag{6}$$

where

$$\Delta V_{\text{sph}i} = \frac{S_i}{4\pi R_i^2}\int_{R_i}^{R_i+\Delta R_i} 4\pi R^2 dR = S_i \Delta R_i \left(1 + \frac{\Delta R_i}{R_i} + \frac{1}{3}\left(\frac{\Delta R_i}{R_i}\right)^2\right); \tag{7}$$

$$\Delta V_i = V_{i+1} - V_i\,; \tag{8}$$

$\dfrac{S_i}{R^2} = \Omega_i$ is the solid angle in which burning from the spherical surface of radius R_i and of area S_i propagates and V_i and V_{i+1} is the volume of the combustion products between the surfaces with subdivision radii R_i and R_{i+1} respectively. Then for the combustion chamber of a prescribed shape we have

$$u_i\,(b_i/d) \cong F_i \frac{\rho_{\text{compr}i}}{\rho_{\text{b}i}}\, u_{\text{n}i}\,. \tag{9}$$

The meaning of expression (9) is as follows: if in propagation of the flame from radius R_i to $R_i + \Delta R_i$ from the surface S_i, the products' volume can diminish F_i times compared to the case of spherical burning, the visible burning velocity u_i in this region will be F_i times higher than that in spherical burning.

The dependences of the velocities u_i corrected with the results of [18, 19] are also presented in Fig. 7b and c. It is seen that the velocity values in the region of up to 0.6 chamber diameter approach experimental values; thereafter calculation yields increasingly more overstated u_i values. Curve 11 of u_i at a high initial pressure has a maximum virtually coincident with the maximum of curve 9 in value but shifted toward the ignition source. An increase in the velocity, which is comparable with the value for curve 5 in amplitude, is observed, as the front approaches the chamber wall; however, the minimum of curve 7 is less pronounced than that of curve 5. On the whole, we can say that correction of the burning velocity using the factor F makes it possible to better describe the behavior of the velocity curves in the first half of the chamber than in its second half. This is, apparently, due to the increasingly larger departure of the burning from the isobaric process in each subsequent layer.

The second burning-velocity maxima are, probably, caused by the development of the instability of the spherical flame front and by the departure of flow from that laminar [20, 21]. The appearance of hills and hollows on the front causes the flame surface to grow; therefore, here the actual value of S (and hence F) becomes substantially higher, which can bring about second velocity maxima.

The rate of rise in the pressure $dP_i/dt = f(t)$ (see Fig. 4c) is one of the most important indices of burning determining the efficiency, power, and economical operation of an engine [22, 23]. The higher this index, i.e., the more actively the mixture burns up, particularly in the final phase of the process, the smaller the advance angle of ignition or injection of the fuel must be set. This leads to the actual process approaching a theoretical one, a decrease in the negative work in the compression stroke, and a reduction in the heat loss to the cylinder walls.

With allowance for what has been said above, the advantages of the synthesis-gas-based mixture (see Fig. 4c, curves 11 and 12) become particularly clear. Calculations show that the energy release in combustion of this mixture is 24% lower than that in the model mixture 1, the maximum values of pressure P_{max} are 12–13% lower, whereas the maximum rates of rise in the pressure exceed the corresponding values in mixture 1 by 2 and 2.6 times at initial values of 0.108 and 0.491 MPa respectively. The rates of rise in the pressure are exceeded at both P_0 values throughout the process of propagation of the flame in the combustion chamber (Fig. 4b–d).

Noteworthy are the curves of change in the dimensionless rates of rise in the pressure $(dP_j/dt)/(dP_j/dt)_{max}$ as the flame front moves along the chamber diameter (Fig. 4b and d). Their behavior is of the same type in character and is independent of the kind of mixture and the initial pressure.

The expression for the rate of rise in the pressure in burning in the spherical bomb has the following form [10]:

$$\frac{dP}{dt} = (P_{max} - P_0)\frac{Su_n\rho_{compr}}{V_{ch}\rho_0}. \quad (10)$$

Here $S = 4\pi R^4$. Then for the chamber of an arbitrary shape with account for (9) we have

$$\left(\frac{dP}{dt}\right)_{b_i} \cong (P_{max} - P_0)\frac{S_i u_i \rho_{bi}}{V_{ch} F_i \rho_0}. \quad (11)$$

In layer (laminar) burning, equal relations b_i/d correspond to nearly equal flame-front surfaces and F_i values; the density of the combustion products ρ_{b_i} is essentially determined by the quantity b_i/d. Furthermore, the form of the distribution of the dimensionless flame velocity u_i/u_{max} is also similar (see Fig. 4b and d). Therefore, in different mixtures, the $(dP_j/dt)/(dP_j/dt)_{max}$ ratios have similar dependences on b_i/d. The observed variations in the dependences of the rates of rise in the pressure are due to the regimes of development of the flame-front instability, which are more conspicuous in more power-intensive stoichiometric mixtures.

Lean Mixtures in Lateral Ignition. Figure 5 gives the velocities of propagation of the flame u_j, the pressures P_j, and the rates of rise in the pressure dP_j/dt in burning of the lean mixtures 2a and 4a as functions of the time and the curves of change in the velocities u_j and dP_j/dt with advance of the flame front. We note the general features of the burning of stoichiometric and lean mixtures: uniform change in the burning velocities with time and along the chamber; decrease in the maximum burning velocity in the model and hydrogen-enriched propane-air mixtures with growth in P_0 and the presence of the second maxima in them at low pressures; a much shorter burning time of the synthesis-gas-based mixture compared to the hydrogen-enriched propane-air mixture. Thus, the realized leaning of the fuels ($\varphi = 0.8$) does not lead to a marked change in the character of burning.

Among the few distinctive features noted in analyzing the behavior of stoichiometric and lean mixtures (see Figs. 4 and 5) is a slight shift of the minima of the burning velocities of the propane-containing mixture toward smaller b/d values at low pressures and a fuller profile of the reduced burning velocity in the case of the synthesis-gas-based lean mixture, where a shelf at a level of 0.55 u/u_{max} is observed in the interval $0.7 \lesssim b/d \lesssim 0.9$.

To infer the scale of the process we present the curves $u_j = f(b/d)$ and $dP_j/dt = f(b/d)$ for mixtures 2a and 4a at $P_0 = 0.491$ MPa in Fig. 5b in natural variables. It is seen that the burning velocities as functions of the position of the front in the synthesis-gas-based mixture are 2–5 times higher that those in the hydrogen-enriched propane-air mixture; the rates of rise in the pressure are higher 3–4 times respectively.

Lean Mixtures in Central Ignition. Figure 6 gives the velocity of propagation of the flame u_j, the pressure P_j and the rate of rise in the pressure dP_j/dt in burning of the lean mixtures 2a and 4a as functions of the time. As for the case of lateral ignition (Fig. 5), we observe a decrease in the burning velocity and a shift of the velocity maximum toward the ignition source with growth in P_0 in the hydrogen-enriched mixture 2a. However, in central ignition, this

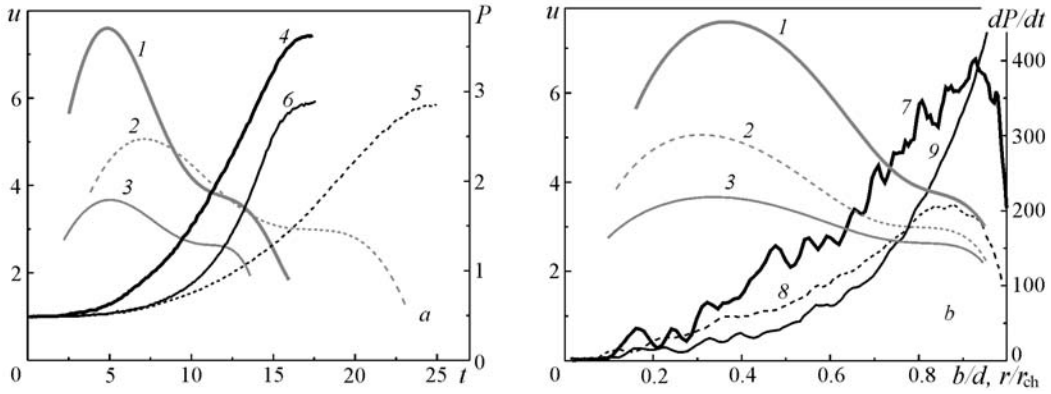

Fig. 8. Curves of change in the flame velocity u (1–3), the pressure P (4–6), and the rate of change in the pressure dP/dt (7–9) in burning of the stoichiometric mixture (1, 4, and 7) and synthesis-gas-based lean mixtures in lateral (2, 5, and 8) and central (3, 6, and 9) ignition with time (a) and along the diameter or on the radius of the chamber (b) at P_0 = 0.491 MPa. t, msec; u, m/sec; P, MPa; dP/dt, MPa/sec.

shift is more pronounced, e.g., as P_0 grows twice (up to 0.196 MPa), the radius of the front with a burning velocity u_{max} diminishes from 14.8 to 9.4 mm in central ignition and from 24.6 only to 22.6 mm in lateral ignition. The tendency for the time of reaching the maximum rate of rise in the pressure $(dP_j/dt)_{max}$ to grow is preserved, as P_0 increases. We note that the times $t_{(dP_j/dt)_{max}}$ diminish with increase in the initial pressure in central ignition in the synthesis-gas-based mixture.

The second feature of burning in central ignition is a different character of behavior of the dP_j/dt curves. Whereas in the first case the rate of rise in the pressure is nearly in proportion to P_0 throughout the process (Fig. 5c), in central initiation, the increase in dP_j/dt at the initial stage of the process is nearly the same at all P_0; for mixtures with a lower pressure, the curves lag behind each other near their maxima, and their descending branches are steeper the higher the initial pressure (Fig. 6e). We note that this character of the time dependences of dP_j/dt in central ignition is also observed in methane-hydrogen-air mixtures (φ = 1 and 0.75) whose fuel consists of 62% methane, 34% hydrogen, and 4% ethylene or is enriched, due to methane, with hydrogen to 44% or ethylene to 8% in the P_0 range from 0.49 to 1.96 MPa [21]. Thus, it is possible that the similarity of the rate of rise in the pressure in central ignition of the mixture with substantial change in P_0 is the characteristic feature of mixtures with a hydrocarbon-hydrogen fuel. We point to the fact that for the model chamber used, closely spaced dP_j/dt values are preserved in mixture 2a at P_0 from 0.098 to 0.491 MPa at least to R = 9 mm, i.e., to a source diameter of about 20 mm.

For the synthesis-gas-based lean mixture (Fig. 6b, d, and f), the distinctions from the behavior of mixture 2a are more numerous than coincidences. The maximum burning velocity is observed at the medium (0.196 MPa) initial pressure, not at the minimum pressure, and is attained at a distance from the plug's interelectrode gap that is the smallest of the three distances rather than at the maximum distance, as in mixture 2a. Once u_{max} have been attained, the velocity values diminish nonmonotonically on the radius; approximately from r/r_{ch} = 0.4–0.5, the burning velocity varies at the level of half its maximum value. The character of behavior of the dP_j/dt curves differs significantly from that described above, too. Without dwelling on the obvious difference in the curves' shape, we note that whereas in mixture 2a, a twofold and fivefold increase in P_0 leads to a growth of only 1.6 and 4 times in $(dP_j/dt)_{max}$, in mixture 4a this growth is 2.5 and 6.5 times respectively.

In connection of the interesting features of the behavior of the synthesis-gas-based mixture, we compare the local characteristics of its burning under different conditions (Fig. 8). Here the burning velocity u_j and the pressure P_j are presented as functions of the time, and the distributions of u_j and dP_j/dt in the chamber (curves 1, 2, and 7, 8, along the diameter; 3 and 9, on the radius) are given. It is seen that the transition from stoichiometric burning to lean burning (φ = 0.8) leads to a decrease of one-third in the maximum burning velocity (curves 1 and 2) and to a twofold decrease in the maximum rate of rise in the pressure (curves 7 and 8). The latter is due to both the decrease in the volume heat of combustion and a growth of 44% in the burning time. The time dependences of pressure in the

TABLE 3. Normal Velocities of Burning of Fuel Mixtures

Fuel mixture	Chemical composition of the mixture	P, MPa	T, K	u_n, m/sec
2a	$0.8C_3H_8 + 0.51H_2 + 5.26O_2 + 19.76N_2$	0.108	301	0.35
		0.204	296	0.32
		0.505	295	0.25
4a	$0.8(CO + 1.33H_2 + 1.88\ N_2) + 1.17O_2 + 4.39N_2$	0.102	297	0.65
		0.202	295	0.82
		0.601	311	0.62

stoichiometric (curve 4) and lean (curve 5) mixtures are identical in character, and the decrease of 21% in the maximum pressure is attributed to the decrease in the volume heat of combustion of the mixture.

Let us consider how the burning velocity changes on transition from lateral ignition to that central. From Fig. 8a, it is clear that its time dependences in mixture 4a (curves 2 and 3) are identical in character; the behavior of curve 1 of the burning velocity of the stoichiometric mixture 4 is similar. The burning-velocity distributions in the chamber are similar, too (Fig. 8b). However, the value of u_{max} is 1.38 times higher in lateral ignition (1.3 times higher for mixture 2a at this pressure and 1.4 times higher for the stoichiometric mixture 1 at 0.098 MPa).

Determination of Normal Burning Velocities. The proposed method of correction of burning velocities makes it possible to relate them for processes approaching spherical burning to variable degrees. An analysis of the dependences of Fig. 7 shows that in the region of maximum burning velocities where the isobaric approximation is the most justified, the burning velocities obtained by different methods, including calculation, from the known value of u_{n0} differ only slightly. Thus, the obtained data enable us to calculate the normal burning velocities of the mixtures under study. Since in central ignition, burning is closer to that spherical, we have performed calculations for this version. The results are presented in Table 3. As is clear from the table, the relation of the normal velocities is close to the relation of the maximum burning velocities of the mixtures. This is not surprising, since the F values changed only from 1.01 to 1.05, and the ratios of the densities entering into expression (8) grew from 7.02 to 7.15 with growth in P_0 in mixture 2a and decreased from 5.91 to 5.65 in mixture 4a. In most versions, the parameters of the compressed mixture were close to the initial ones.

On the Structure and Surface Area of the Flame. A comparison of the character of burning of the synthesis-gas-based mixture and the hydrogen-enriched propane-air mixture shows that the significant difference in the integral and local characteristics of burning for these mixtures can be due to the cellular flame structure recorded in the synthesis-gas-based mixture and leading to an increase in the burning surface, which is produced by the local bends of the spherical front. The above growth in the burning surface can be evaluated indirectly using expression (11). The indices of burning entering in (11) are given in Table 2; the densities ρ_{0i} are determined from the composition of the mixtures and the initial conditions; V_{ch} = const; the values of the shape factor F_{ij} are equal when subdivision of the chamber into regions is identical, and knowing the pressure distribution in the chamber, we can determine the distribution of the combustion-product densities $\rho_{b_{ij}}$. Then the expression for the surface ratio takes the form

$$\frac{S_{4a}(r_i/r_{ch})}{S_{2a}(r_i/r_{ch})} = A \frac{\left(\frac{dP}{dt}\right)_{4a}}{\left(\frac{dP}{dt}\right)_{2a}} \frac{\rho_{b2a_i}}{\rho_{b4a_i}} \frac{u_{2a_i}}{u_{4a_i}}, \tag{12}$$

where $A = \dfrac{\rho_{0_{4a}}(P_{max_{2a}} - P_0)}{\rho_{0_{2a}}(P_{max_{4a}} - P_0)}$.

Figure 9 shows the dependences of the ratios $S_{4a_i}/S_{2a_i}(r/r_{ch})$ and $S_{4a_i}/S_{2a_i}(b/d)$, which have been obtained with this procedure of processing and calculation. It is seen that despite the substantial variations of the values, the flame-surface ratios are close to unity as a rule. The significant difference in the initial values of $S_{4a_i}/S_{2a_i}(r/r_{ch})$ at

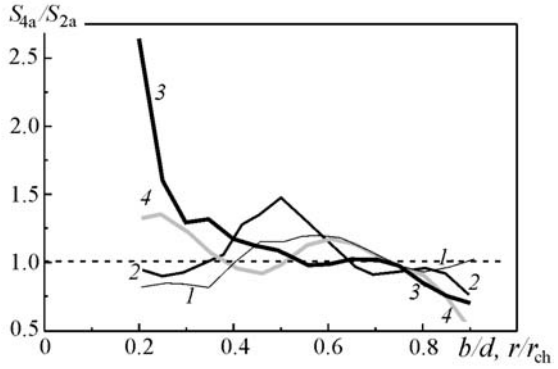

Fig. 9. Ratio of the flame surfaces in the synthesis-gas-based mixture and in the propane-air mixture enriched with 2% hydrogen in propagation of burning in the chamber in the case of central (1–3) and lateral (4) ignition of lean mixtures (φ = 0.8) at an initial pressure of 0.098 (1), 0.196 (2), and 0.491 MPa (3 and 4).

P_0 = 0.491 MPa in the case of central ignition is attributable to the large error in determining the position of the combustion fronts in the compared mixtures near the site of ignition. With the total error in determining the position of the fronts $\Delta r = \left|R_{2a_i} - R_{4a_i}\right|$ = 2 mm, the ratio of purely spherical front surfaces may attain a value of 1.8 for r/r_{ch} = 0.2, 1.2 for r/r_{ch} = 0.5, and 1.1 for r/r_{ch} = 0.8. Thus, the reliability of the calculation results must improve with growth in the dimension of the regions of burning. Therefore, it is evident that the convergence of the curves for different P_0 when $r/r_{ch} \geq 0.6$ is a reflection of the actual regularities of the processes, and the $S_{4a_i}/S_{2a_i}(r/r_{ch})$ values close to unity in the region $0.6 \lesssim r/r_{ch} \lesssim 0.8$ may be considered an established fact.

Conclusions. We have studied the burning of a propane-air mixture and its hydrogen-enriched (with 2 and 4%) modifications and of mixtures based on propane-conversion products in the cylindrical chamber in the range of the initial pressures 0.024–1 MPa and at an initial temperature of 290–300 K for the stoichiometric coefficients φ = 1.0 and 0.8 in the cases of lateral and central initiation.

It has been shown that in the range of initial pressures of 0.1 to 1 MPa, the burning times of the propane-air mixtures and their hydrogen-enriched modifications grow almost linearly (by 33% in the stoichiometric mixture and by 74% in the lean mixture with a growth of 8 times in P_0 in the propane-air mixtures); hydrogen enrichment intensifies the process of burning, more substantially in lean mixtures. Thus, at P_0 = 0.8 MPa, addition of 4% hydrogen causes the burning time of the stoichiometric mixture to decrease 1.25 times and even 1.7 times when φ = 0.8. The burning of the synthesis-gas-based mixtures is much faster that that of the propane-air mixture and its hydrogen-enriched modifications; when φ = 1, the burning time of the synthesis-gas-based mixture is 2.2–2.8 times shorter than that of the propane-air mixture. Furthermore, it depends almost not at all on the mixture's initial pressure in the combustion chamber.

We have obtained the dependences of the burning velocity $u(t)$ and the u distributions in the chamber in the range of the initial pressures 0.1–0.5 MPa in stoichiometric and lean mixtures. The local characteristics of burning of the model propane-air mixture and its molecular-hydrogen-enriched (with 2 and 4% due to air) modifications and of the propane-conversion products (synthesis-gas-based mixtures) in the pressure range 0.1–0.5 MPa and at an initial temperature of 290–300 K and stoichiometric coefficients φ = 1.0 and 0.8 have been determined.

It has been shown that the burning times in central ignition in all mixtures are shorter then those in lateral ignition; the u_{max} values in the latter case are always higher. We have proposed the procedure of correction of the values of the velocities u, which is based on subdivision of the chamber into regions and determination, for each, of the shape factor F_i characterizing the distribution of burning in a region from the spherical burning. The corrected u_i values for the model stoichiometric mixture satisfactorily agree with experimental burning velocities.

We have determined the velocities of normal burning of lean mixtures in the pressure range 0.1–0.6 MPa at their temperatures of about 300 K. It has been shown that the velocities in the hydrogen-enriched propane-air mixture drop with initial pressure; in the synthesis-gas-based mixture, the maximum normal velocity (0.82 m/sec) is observed at P_0 = 0.2 MPa.

We have obtained the dependences of the rates of rise in the pressure dP/dt on time and the distributions of dP/dt in the chamber in the stoichiometric and lean mixtures. The maximum rates of rise in the pressure are observed at the end of the process, when the radii of the combustion fronts and the densities of the adiabatically compressed mixture are nearly maximum. On transition from the lateral ignition to that central, the dP/dt values grow 2.4 times in the investigated mixtures.

On the basis of a set of data on the distributions of the rates of rise in the pressure, the burning velocities, and the pressures in the chamber, we have compared the flame surfaces in the synthesis-gas-based mixture and the propane-air mixture enriched with 2% hydrogen. It has been shown that in the chamber region where $0.6 \lesssim r/r_{ch} \lesssim 0.8$, the flame-surface ratios are close to unity. Thus, the presence of the cellular structure of the flame of the synthesis-gas-based mixture does not lead to a marked growth in the flame surface in this region of the chamber.

NOTATION

b, (diametral) distance between the combustion front and the wall next to the lateral plug, mm; d, chamber diameter, mm; g and f, functions; F, shape factor; m, parameter; P, pressure, MPa; R, flame-front radius, mm; r, running coordinate of the front, mm; S, burning surface (area), mm^2; T, temperature, K; t, time, sec; u, burning velocity, m/sec; u_n, normal-burning velocity, m/sec; V, volume, mm^3; ρ, density, kg/m^3; φ, stoichiometric coefficient; Ω, solid angle, sr. Subscripts: b, burning, combustion; ch, chamber; eq, equilibrium; compr, compressed fresh mixture; i, subdivision region; j, mixture; max, maximum; 0, initial; n, normal; sph, sphere.

REFERENCES

1. G. D. Berry, A. D. Pasternak, G. D. Rambach, J. R. Smith, and R. N. Schock, Hydrogen as a future transportation fuel, *Energy*, **21**, No. 4, 289–303 (1996).
2. M. A. Brown, M. D. Levine, W. Short, and J. G. Koomey, Scenarios for a clean energy future, *Energy Policy*, **29**, 1179–1196 (2001).
3. T. D. Andrea, P. F. Henshaw, and D. S.-K. Ting, The addition of hydrogen to a gasoline-fueled S.I. engine, *Int. J. Hydrogen Energy*, **29**, 1541–1552 (2004).
4. C. G. Bauer and T. Forest, Effect of hydrogen addition on performance of methane-fueled vehicles. Part I: Effect on S.I. engine performance, *Int. J. Hydrogen Energy*, **26**, 71–90 (2001).
5. A. N. Migun, A. P. Chernukho, and S. A. Zhdanok, Influence of the addition of hydrogen and of a synthesis gas on the characteristics of the process of combustion of gasoline-air mixtures under conditions typical of internal combustion engines, *Inzh.-Fiz. Zh.*, **79**, No. 4, 23–28 (2006).
6. D. Lewis and G. von Elbe, *Combustion, Flames and Explosions in Gases*, Academic Press, New York (1961).
7. V. N. Kondrat'ev and E. E. Nikitin, *Chemical Processes in Gases* [in Russian], Nauka, Moscow (1981).
8. M. Assad, V. V. Leshchevich, V. N. Mironov, O. G. Penyazkov, and K. L. Sevruk, Combustion of modified fuels in the model of the ICE combustion chamber, in: *Heat and Mass Transfer–2005* [in Russian], ITMO im. A. V. Lykova, NAN Belarusi, Minsk (2005), pp. 100–105.
9. M. Assad, V. V. Leshchevich, V. N. Mironof, O. G. Penyazkov, K. L. Sevruk, and A. V. Skilond, Combustion of hydrogen-contained fuels in the model of ice chamber, *Int. Workshop "Nonequilibrium Processes in Combustion and Plasma Based Technologies,"* 26–31 August, Minsk (2006), pp. 124–129.
10. E. S. Shchetinkov, *Physics of the Combustion of Gases* [in Russian], Nauka, Moscow (1965).
11. Ya. K. Troshin and K. I. Shchelkin, Structure of the front of spherical flames and instability of normal combustion, *Izv. Akad. Nauk SSSR*, No. 9, 160–166 (1955).
12. L. A. Gussak, E. N. Sprintsina, and K. I. Shchelkin, Investigation of the normal-flame-front stability, *Fiz. Goreniya Vzryva*, **4**, No. 3, 358–366 (1968).
13. V. P. Karpov, A. Yu. Kusharin, O. E. Popov, and B. E. Gel'fand, Experimental observations and numerical simulation of combustion in lean H_2–CO–air mixtures in a spherical bomb, in: *Chemical Physics of the Processes of Combustion and Explosion*, *12th Symposium on Combustion and Explosion*, Chernogolovka (2000), Pt. 1, pp. 72–74.

14. O. E. Popov, V. P. Karpov, B. E. Gelfand, and S. V. Khomik, Combustion and explosion characteristics of H_2–CO–air mixtures, in: *Proc. 3rd Asia-Pacific Conf. on Combustion*, Seoul, Korea (2001), pp. 730–733.
15. R. J. Kee, F. M. Rupley, E. Meeks, and J. A. Miller, *Chemkin-III: A Fortran Chemical Kinetics Package for the Analysis of Gas-Phase Chemical and Plasma Kinetics*, Sandia National Laboratories Report SAND96-8216 (1996).
16. A. A. Konnov, Detailed reaction mechanism for small hydrocarbons combustion. Release 0.5.1998. http://homepages.vub.ac,be/~ akonnov.
17. S. A. Gol'denberg and V. S. Pelevin, Influence of pressure on the rate of flame propagation in a laminar flow, in: *Investigation of Combustion Processes* [in Russian], Izd. Akad. Nauk SSSR, Moscow (1958), pp. 57–67.
18. M. S. Assad, V. N. Mironov, and O. G. Penyazkov, On calculation of the running volume of combustion products in a cylindrical vessel, *Mekh. Mash.*, *Mekhanizm.*, *Mater.*, No. 2 (3), 52–57 (2008).
19. M. S. Assad, V. N. Mironov, and O. G. Penyazkov, Modeling of the flame surface area during combustion in a closed vesel, *Mekh. Mash.*, *Mekhanizm.*, *Mater.*, No. 1 (2), 60–65 (2008).
20. B. Ya. Zel'dovich, G. I. Barenblatt, V. B. Librovich, and G. M. Makhviladze, *Mathematical Theory of Combustion and Explosion* [in Russian], Nauka, Moscow (1980).
21. B. E. Gel'fand, M. V. Sil'nikov, S. P. Medvedev, and S. V. Khomik, *Thermogasdynamics of the Combustion and Explosion of Hydrogen* [in Russian], Politekh. Univ., St. Petersburg (2009).
22. P. Kh. D'yachenko (Ed.), *Theory of Internal Combustion Engines* [in Russian], Mashinostroenie, Leningrad (1977).
23. A. V. Nikolaenko, *Theory*, *Construction*, *and Computation of Automobile and Tractor Engines* [in Russian], Kolos, Moscow (1984).
24. M. S. Assad, V. V. Leshchevich, V. N. Mironov, O. G. Penyazkov, K. L. Sevruk, and A. V. Skilond', Combustion of methane-hydrogen-air mixtures in the model of the internal combustion engine chamber, in: *Heat and Mass Transfer-2007*, A. V. Luikov Heat and Mass Transfer Institute, National Academy of Sciences of Belarus, Minsk (2007), pp. 65–71.